Review

An Overview of Fatigue Testing Systems for Metals under Uniaxial and Multiaxial Random Loadings

Julian M. E. Marques [1,*] **, Denis Benasciutti** [1,*] **, Adam Niesłony** [2] **and Janko Slavič** [3]

1   Department of Engineering, University of Ferrara, Via Saragat 1, 44122 Ferrara, Italy
2   Department of Mechanics and Machine Design, Faculty of Mechanical Engineering,
     Opole University of Technology, Prószkowska 76, 45-758 Opole, Poland; a.nieslony@po.edu.pl
3   Faculty of Mechanical Engineering, University of Ljubljana, Aškerčeva 6, 1000 Ljubljana, Slovenia;
     janko.slavic@fs.uni-lj.si
*   Correspondence: nzvjnm@unife.it (J.M.E.M.); denis.benasciutti@unife.it (D.B.);
     Tel.: +39-0532-974104 (J.M.E.M.); +39-0532-974976 (D.B.)

Abstract: This paper presents an overview of fatigue testing systems in high-cycle regime for metals subjected to uniaxial and multiaxial random loadings. The different testing systems are critically discussed, highlighting advantages and possible limitations. By identifying relevant features, the testing systems are classified in terms of type of machine (servo-hydraulic or shaker tables), specimen geometry and applied constraints, number of load or acceleration inputs needed to perform the test, type of loading acting on the specimen and resulting state of stress. Specimens with plate, cylindrical and more elaborated geometry are also considered as a further classification criterion. This review also discusses the relationship between the applied input and the resulting local state of stress in the specimen. Since a general criterion to classify fatigue testing systems for random loadings seems not to exist, the present review—by emphasizing analogies and differences among various layouts—may provide the reader with a guideline to classify future equipment.

Keywords: fatigue; testing systems; random loadings; servo-hydraulic; shaker table

1. Introduction

Mechanical components are often subjected to random loadings during their service life. Due to these loads, components may be exposed to a local random stress, which can be uniaxial (i.e., only one stress component) or multiaxial (i.e., two or more stress components). To estimate the component life, engineers usually perform a structural durability assessment in the predesign stage, often with the aid of a finite element (FE) analysis.

If the nodal random stress is uniaxial, the approach commonly followed makes use of rainflow counting and the Palmgren–Miner rule to compute the damage of the nodal stress output, based on uniaxial strength data given as an S–N curve. This analysis can be developed in time domain or, equivalently, in frequency domain [1].

If, instead, the nodal stress in the FE model is multiaxial, the analysis requires the use of a multiaxial fatigue criterion, which can also be formulated in time domain or frequency domain [2]. By analyzing all nodal results of a FE model (e.g., hundreds of thousands), the computation time is very long using a time-domain criterion. In addition, it may become impracticable when a huge number of planes have to be scanned in the whole three-dimensional FE model in the case of multiaxial fatigue criteria using the critical plane concept [3–5]. In general, for both the uniaxial and multiaxial cases, frequency domain solutions are several orders of magnitude faster than time domain simulations [6–9].

Methods for durability analysis, either in time domain or frequency domain, have to rely on material strength data obtained by experimental laboratory tests. Such tests are performed by applying loadings on a specimen, where cracks nucleate and grow until the specimen breaks. Tests with simple loadings (e.g., axial, bending and torsion) are carried

out to estimate the material fatigue strength data in the uniaxial case. These uniaxial tests yield an S–N curve in high-cycle fatigue regime, which characterizes the material strength behavior in terms of amplitudes versus number of cycles to failure. Uniaxial test data are also necessary for calibrating a multiaxial criterion. Once calibration has been carried out, specific tests with multiaxial loadings (e.g., bending and torsion) are also performed to gather the necessary data for validating the multiaxial criterion. It is, nevertheless, clear that systems and methodologies for fatigue testing play a paramount role in the durability analysis of both uniaxial and multiaxial states of stress.

Fatigue testing methodologies may vary, for instance, in terms of type of machine used. Two different types (servo-hydraulic or electrodynamic shaker tables) are usually adopted in laboratories. Although, in general, servo-hydraulic machines can be used with both plate and cylindrical specimens, they are normally employed with cylindrical specimens in the random fatigue testing methodologies addressed in this paper. By contrast, shaker tables also adopt specimen geometries other than cylindrical, for example, plate or more elaborated ones.

Various specimen geometries and layouts are considered in fatigue tests, too. While the use of servo-hydraulic machines or shaker tables sometimes leads to rather simple testing layouts or state of stress (e.g., uniaxial), in some cases, the testing systems are all but obvious. As an example, a widely used system layout is that considering a cantilever plate specimen with rectangular shape [10–14]. Mounted on shaker tables and excited at its base, this system produces a bending random loading, which results in a near uniaxial state of stress in the critical location (e.g., notch or hole). However, using a different system with a cantilever cylindrical specimen, it is possible to reach a biaxial state of stress with both normal and shear stresses [15]. Applying loads at the free end of the specimen by a uniaxial shaker allows the system only to develop a coupled bending–torsion random loading. To overcome this limitation, bending and torsion can be applied by two independent uniaxial shakers [15]. In this case, not only coupled (correlated) but also uncoupled (uncorrelated) bending–torsion random loadings are achieved.

Another interesting system with a cantilever cylindrical specimen is that using two masses of different weights fixed at the free end [16]. Excited by a uniaxial shaker at its base, this specimen experiences a bending–torsion loading that produces coupled normal and shear stress components. Inspired by this layout, a new testing system was designed to apply only bending or torsion, as well as coupled or uncoupled bending–torsion loadings by a tri-axis shaker [17–19]. This system permits the intensity and phase shift of bending and torsion loadings to be controlled independently, which results in local normal and shear stresses with any degree of correlation. Experimental and numerical analyses confirmed the system's behavior.

A more elaborated specimen with Y-shaped geometry was also proposed not only to accelerate fatigue tests by means of shaker tables but also to simulate a real-world scenario of complex structures [20–25]. Although this special Y-shaped system is excited by two uncoupled random loadings (in vertical and horizontal directions), it develops a biaxial state of stress at the critical location in terms of normal stresses.

As may be expected, and perhaps become more apparent in the following sections, performing tests with a uniaxial stress is much easier than executing tests with a biaxial stress, even if one makes use of a bending–torsion servo-hydraulic machine. The degree of complexity of the testing system increases the most when the biaxial state of stress is random. While a uniaxial stress can be achieved simply by a servo-hydraulic machine with axially loaded specimens, or by a uniaxial shaker table with a cantilever specimen, fatigue tests in a biaxial random state of stress require one or more machines (e.g., one tri-axis shaker or two uniaxial shakers), one or more types of input as force/torque or acceleration, a specific testing layout and/or a particular shape of specimen. Although it is true that carrying out a fatigue test with a biaxial state of stress is not as simple as executing a test with uniaxial stress, the interest in biaxial random fatigue tests has increased in the last decade in the scientific community [15,17–25].

By considering this increased interest, the present paper aims to review the random loading fatigue testing systems available in the literature. The different testing systems are critically discussed, highlighting advantages and possible disadvantages. Some general features are also identified, which allow testing systems to be classified and grouped in terms of type of testing machine, specimen geometry, applied constraints, type and among of input needed to carry out a fatigue test, type of random loadings acting on the specimen and the resulting local state of stress. Regarding the loadings applied on specimens in fatigue tests, this paper focuses on axial, bending, torsion, axial-torsion and bending–torsion loadings. Specimens subjected to such loadings yield a uniaxial or a biaxial state of stress, which is also discussed hereafter.

Finally, it must be emphasized that, although testing systems for fatigue random loading are reviewed in detail throughout the text, the relationship between experimental results and estimations by various multiaxial fatigue criteria—though interesting—is not the scope of the present paper. For a discussion on this topic, the reader may refer to [26,27].

2. Common Random Loadings in Fatigue Tests and Resulting State of Stress

A multiaxial state of stress at a critical point of a mechanical component is represented by a tensor $\sigma(t)$, which in the most general case has six independent stress components [28]. For this reason, the six independent stress components are conveniently arranged into a six-dimensional vector $s(t) = \left[\sigma_{xx}(t), \sigma_{yy}(t), \sigma_{zz}(t), \tau_{xy}(t), \tau_{yz}(t), \tau_{zx}(t)\right]$, where $\sigma_{xx}(t)$, $\sigma_{yy}(t)$ and $\sigma_{zz}(t)$ are normal stresses and $\tau_{xy}(t)$, $\tau_{yz}(t)$ and $\tau_{zx}(t)$ are the shear stresses in an X–Y–Z cartesian coordinate system.

Usually, fatigue cracks nucleate at the surface of mechanical components, where the local state of stress is biaxial or even uniaxial. Therefore, in laboratory fatigue tests, the aim is to replicate in a specimen the same biaxial or uniaxial state of stress, in which only two or less normal stress components are nonzero [26,28]. While, in plane stress, a biaxial stress may have up to three nonzero components, $\sigma_{xx}(t)$, $\sigma_{yy}(t)$ and $\tau_{xy}(t)$, special cases often employed in laboratory tests consider one normal $\sigma_{xx}(t)$ and one shear $\tau_{xy}(t)$ stress, or nonzero normal stresses in two directions $\sigma_{xx}(t)$, $\sigma_{yy}(t)$. The uniaxial cases frequently adopted refer to a pure normal stress $\sigma_{xx}(t)$ or shear stress $\tau_{xy}(t)$; see Figure 1.
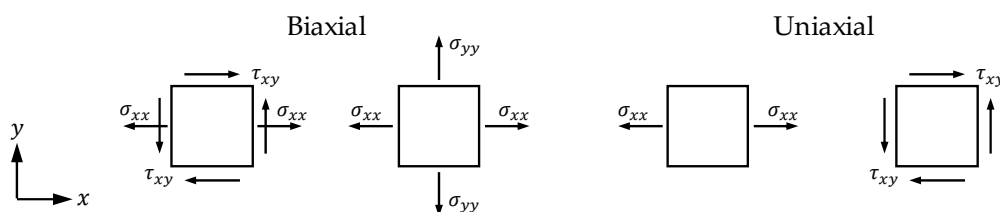

Figure 1. Common state of stress in fatigue testing: biaxial (e.g., normal and shear stresses or normal stresses in two directions); uniaxial (e.g., pure normal stress or pure shear stress).

In tests with constant amplitude loadings, it is common to use harmonic (sinusoidal) functions. For example, a biaxial normal shear stress with zero-mean is:

$$\sigma_{xx}(t) = \sigma_{xx,a}\sin(\omega t), \quad \tau_{xy}(t) = \tau_{xy,a}\sin(\omega t - \varphi) \tag{1}$$

where ω is the angular frequency and $\sigma_{xx,a}$ and $\tau_{xy,a}$ are the stress amplitudes.

For this biaxial state of stress (as, in fact, in any multiaxial case), the magnitude of stress components may change proportionally (in-phase) or nonproportionally (out-of-phase) with time. In particular, the ratio between normal and shear stresses, $\sigma_{xx}(t)/\tau_{xy}(t)$, at any time instant does not vary if $\varphi = 0$, and both stresses follow two in-phase harmonic functions. Instead, the ratio varies with time if $\varphi \neq 0$ and the two harmonic functions are out-of-phase. Additionally, the orientation of principal stress directions may change or not, depending on the value of φ: for in-phase stresses, they remain fixed; for out-of-phase stress, they change with time.

For harmonic stresses with the same frequency, the phase shift φ provides a simple measure of the degree of nonproportionality. This definition cannot be extended to random stresses, as they can be viewed as a superposition of many harmonic functions with different frequencies and phase shifts. In the random case, a statistical approach is needed to express the concepts of "fully correlated", "partially correlated" or "not correlated" (uncorrelated) signals. To this end, one introduces the so-called correlation coefficient between two random stresses, which is defined as the covariance normalized to the standard deviation (see below).

In tests with multiaxial random loadings, each stress component is a zero-mean stationary Gaussian process, which can be characterized in the frequency domain by a Power Spectral Density (PSD) matrix. For a biaxial random stress, $\sigma_{xx}(t)$, $\sigma_{yy}(t)$ and $\tau_{xy}(t)$, the PSD matrix takes the form [9,29]:

$$S(\omega) = \begin{bmatrix} S_{xx,xx}(\omega) & S_{xx,yy}(\omega) & S_{xx,xy}(\omega) \\ S^*_{xx,yy}(\omega) & S_{yy,yy}(\omega) & S_{yy,xy}(\omega) \\ S^*_{xx,xy}(\omega) & S^*_{yy,xy}(\omega) & S_{xy,xy}(\omega) \end{bmatrix}, \quad S_{ij}(\omega) = \int_{-\infty}^{\infty} R_{ij}(\delta)e^{-i\omega\delta}\,\mathrm{d}\delta \quad (2)$$

in which $R_{ij}(\delta)$ is the autocorrelation (for $i = j$) and cross-correlation (for $i \neq j$) function in time-domain, and δ is a time lag. The diagonal terms of $S(\omega)$ are the auto-PSDs $S_{xx,xx}(\omega)$, $S_{yy,yy}(\omega)$ and $S_{xy,xy}(\omega)$, whereas the out-of-diagonal terms are the cross-PSDs $S^*_{xx,yy}(\omega)$, $S^*_{xx,xy}(\omega)$ and $S^*_{yy,xy}(\omega)$, where the superscript * denotes the complex conjugate. Hence, the cross-PSDs are the summation of a real and an imaginary part. The real part is an even function of ω (coincident spectrum or co-spectrum), and the imaginary part is an odd function of ω (quadrature spectrum or quad-spectrum). The PSD matrix in Equation (2) is Hermitian.

Thanks to the relationship between covariance terms and the zero-order spectral moments, $C_{ij} = \lambda_{0,ij}$, the covariance matrix can be defined as [29]:

$$C = \begin{bmatrix} C_{xx,xx} & C_{xx,yy} & C_{xx,xy} \\ C_{yy,xx} & C_{yy,yy} & C_{yy,xy} \\ C_{xy,xx} & C_{xy,yy} & C_{xy,xy} \end{bmatrix}, \quad C_{ij} = \int_{-\infty}^{\infty} S_{ij}(\omega)\,\mathrm{d}\omega \quad (3)$$

Equation (3) is a symmetric matrix. The main diagonal terms are the variance of each stress component, $C_{xx,xx} = \mathrm{Var}(\sigma_{xx}(t))$, $C_{yy,yy} = \mathrm{Var}(\sigma_{yy}(t))$ and $C_{xy,xy} = \mathrm{Var}(\tau_{xy}(t))$; the out-of-diagonal terms are the covariance of two components, $C_{xx,yy} = \mathrm{Cov}(\sigma_{xx}(t), \sigma_{yy}(t))$, $C_{xx,xy} = \mathrm{Cov}(\sigma_{xx}(t), \tau_{xy}(t))$ and $C_{yy,xy} = \mathrm{Cov}(\sigma_{yy}(t), \tau_{xy}(t))$. The covariances are used to define the correlation coefficient $r_{ij} = C_{ij}/\sqrt{C_{ii}C_{jj}}$ between stress components i and j. This coefficient is close to unity when two components are "fully correlated" (proportional); it tends to zero when they are "uncorrelated" (nonproportional) [29].

In some testing layouts, the type of local random stress in the specimen (e.g., biaxial normal and shear stresses $\sigma_{xx}(t)$, $\tau_{xy}(t)$) closely depends on the type of machine, specimen geometry, constrains, and type of excitation. For example, a cantilever cylindrical specimen with a circumferential notch can be subjected to various independent types of loadings applied at the free end, see Figure 2. In the most general case, they are axial load $P(t)$; torsion $M_T(t)$; and two bending moments, $M_{B,x}(t)$ and $M_{B,y}(t)$,, in two orthogonal planes. For this specimen geometry, the maximum stresses are located on the surface at the center of the notch.

Assuming a bending–torsion loading, $M_{B,x}(t)$ and $M_T(t)$, without $P(t)$ and $M_{B,y}(t)$, the cylindrical specimen experiences a biaxial normal and shear stress at the critical location. By contrast, the specimen under the two bending moments $M_{B,x}(t)$ and $M_{B,y}(t)$ develops a uniaxial normal stress at the notch surface. The location of the maximum normal stress changes or not, depending on whether the instantaneous value $M_{B,y}(t)/M_{B,x}(t)$ varies or not.
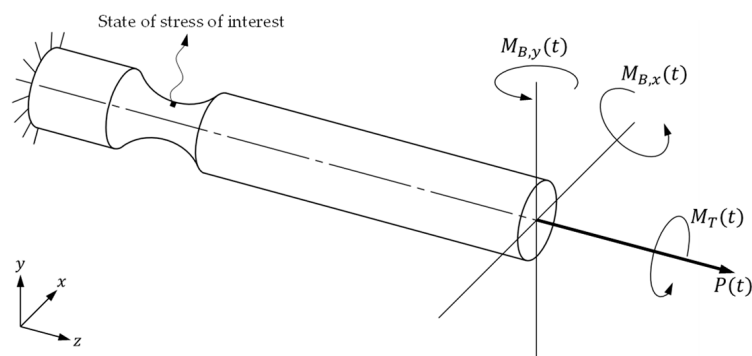
Figure 2. Notched cantilever cylindrical specimen under axial $P(t)$; torsion $M_T(t)$; and two bending moments, $M_{B,x}(t)$ and $M_{B,y}(t)$, applied at the free end.

If the cylindrical specimen in Figure 2 undergoes bending $M_{B,x}(t)$ and torsion $M_T(t)$ moments, it is straightforward to determine the elastic peak normal and shear stresses as [30]:

$$\sigma_{z,p}(t) = \frac{32\,M_{B,x}(t)}{\pi d^3}K_{t,B}, \quad \tau_{xy,p}(t) = \frac{16\,M_T(t)}{\pi d^3}K_{t,T} \tag{4}$$

where d is the specimen diameter in the smallest section, and $K_{t,B}$ and $K_{t,T}$ are the stress concentration factors in bending and torsion. Equation (4) makes apparent how the local stress is directly proportional to the applied loadings. Moreover, it also highlights the role of the stress concentration factors, $K_{t,B}$ and $K_{t,T}$, in increasing the local stress.

Another common layout often exploited in fatigue tests is that in which the specimen is excited at its base. Figure 3 illustrates a cantilever cylindrical specimen, subjected to two orthogonal accelerations, $\ddot{y}(t)$ and $\ddot{x}(t)$, at the clamped end. Both accelerations make the specimen vibrate in bending. In most cases, though, only the vertical acceleration is applied.
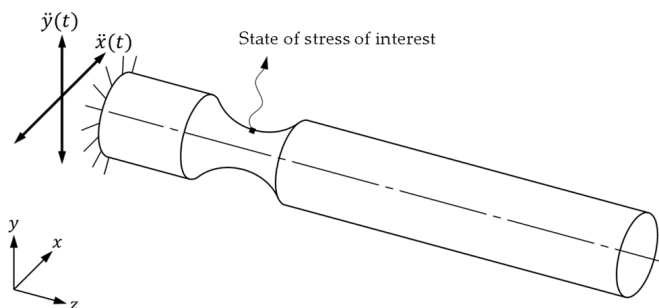

Figure 3. Notched cantilever cylindrical specimen subjected to orthogonal base accelerations $\ddot{y}(t)$ and $\ddot{x}(t)$.

In this testing layout, a modal analysis is normally carried out to identify the modes of vibration and the natural frequencies of the specimen [9]. Usually, the input acceleration is tuned at the first specimen natural frequency. Based on the harmonic analysis, the dynamic response (e.g., stress) of the system is associated to the excitation (e.g., force or acceleration); here, special care is required for kinematic excitation as the natural dynamics changes if compared to the force/dynamics excitation [9].

Assuming a time-invariant linear system, simple relationships exist between the input acceleration and the resulting local stress. For example, for a harmonic vertical acceleration $\ddot{y}(t) = a_y \cos(\omega)$ with amplitude a_y and frequency ω centered on the first resonance frequency of the specimen, the corresponding peak stress is also harmonic with same frequency and amplitude:

$$(\sigma_{z,p})_a = |H_\sigma(\omega)| \cdot a_y \tag{5}$$

where $H_\sigma(\omega)$ is the frequency transfer function for bending. Similar relations hold for other nonzero stress components, if present. For example, an eccentric (off-set) tip mass mounted on the specimen in Figure 3 would also determine a torsional deformation of the specimen, with a corresponding shear stress at the notch. The amplitude of the peak shear stress then would be $\left(\tau_{xy,p}\right)_a = |H_\tau(\omega)| \cdot a_y$, where $H_\tau(\omega)$ is the frequency transfer function in torsion.

The previous relations can be generalized to the case of a specimen under random base accelerations:

$$S(\omega) = H(\omega)S_a(\omega)H^{*T}(\omega) \tag{6}$$

where $S_a(\omega)$ is the PSD matrix of the input accelerations, $H(\omega)$ the frequency transfer function matrix characterizing the system, and $S(\omega)$ is the PSD matrix of the stress, defined in Equation (2). The matrix $S_a(\omega)$ specifies the frequency content and correlations of the random accelerations applied to the specimen, in terms of auto- and cross-PSDs.

Before carrying out the tests, one has to carefully establish the relationship between the type and number of random loadings applied to a specimen and the resulting state of stress at the critical point. Not always does a multiaxial input determine a multiaxial state of stress. In some circumstances, a testing system under a multiaxial input develops a uniaxial stress [31,32]. An alternative to verify the state of stress evaluated theoretically or numerically (e.g., results obtained by FE analysis) is by means of strain gages. Although some specimens have a complex notched geometry that makes it difficult, if not impossible, to attach strain gages directly at the notch, they allow the local stress to be assessed indirectly through strains measured in other points of either the specimen or the testing system [17–19].

In addition to the external random loadings and the state of stress of interest, the choice of the testing machine also offers advantages and disadvantages when performing the fatigue tests; they are discussed in the next section.

3. Fatigue Testing Machines

Two different types of testing machines are usually adopted in mechanical laboratories to perform fatigue tests with random loading. They are known as servo-hydraulic, Figure 4a, and electrodynamic shaker tables, Figure 4b. Servo-hydraulic machines impose a force and/or torque as the input excitation, while electrodynamic shakers apply a force to the vibrating table (where the acceleration is usually controlled with a closed-loop control).
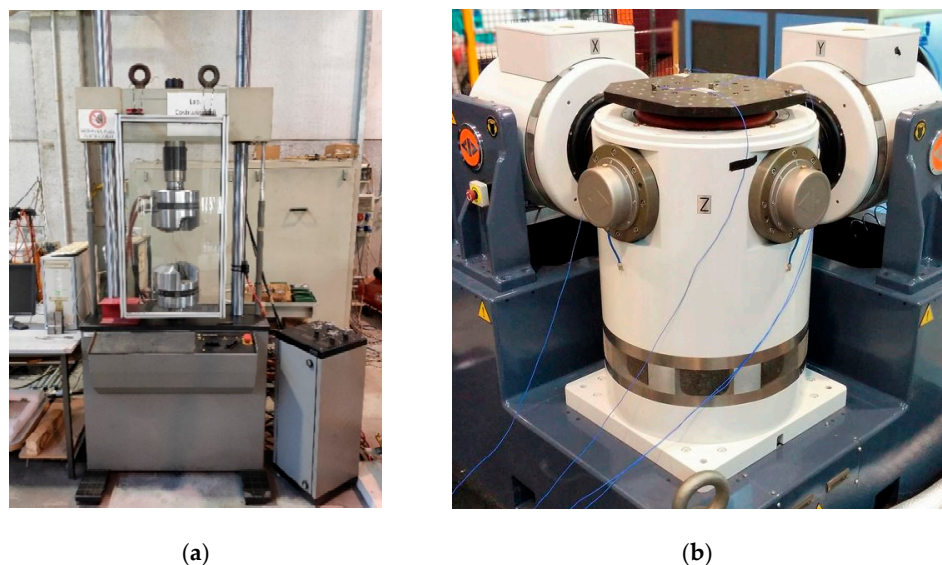

(**a**)　　　　　　　　　　　　　　　　　　　　　(**b**)

Figure 4. Testing machines adopted in mechanical laboratories: (**a**) servo-hydraulic; (**b**) electrodynamic shaker table.

Electrodynamic shakers have a great advantage in that they allow their table to be driven at high frequencies. Consequently, fatigue tests by shaker tables take much less time than tests by servo-hydraulic machines. On the other hand, in servo-hydraulic machines, the force or torque applied to the specimen is controlled directly by the control system; this permits the local state of stress in the specimen to be related directly to the applied loadings, see, for example, Equation (4). With electrodynamic shakers, instead, the local state of stress depends on the dynamic response of the test specimen. Carrying out a dynamic analysis to estimate the local stress in the specimen is, therefore, of considerable importance before performing fatigue tests with shaker tables.

With a uniaxial electrodynamic shaker, a specimen can easily be subjected to a random bending when excited by a vertical base acceleration; see Figure 3. However, by an appropriate setup [17–19], electrodynamic shakers can also be used for tests with bending–torsion random loadings, which result into biaxial normal and shear stresses, $\sigma_{xx}(t)$ and $\tau_{xy}(t)$. This type of bending–torsion loading is not commonly found in tests with a servo-hydraulic machine. In fact, biaxial servo-hydraulic machines can normally apply axial-torsion loading to produce a biaxial state of stress $\sigma_{xx}(t)$, $\tau_{xy}(t)$.

Servo-hydraulic machines, on the other hand, have a greater flexibility in controlling the amplitude and phase of axial-torsion loadings. In the case of fatigue testing with shaker tables, bending–torsion loadings are reached by a more complex system configuration, and their values are not controlled directly by the system. This restriction may pose some difficulty in determining the actual values of the local state of stress that is obtained in the specimen. For this reason, in applications with shaker tables, it is also important to monitor accelerations and strains. Accelerometers are often used to control the acceleration imposed on the table and the dynamic response of the system. Strain gages are employed for measuring and controlling strain at the point of maximum stress, or nearby in case it is not directly accessible. Strain gages are attached on the specimen close to a notch or hole, or on the clamping system to provide an indirect measure of the stress in the specimen.

In electrodynamic shaker tests, the fixation of the sample to the shaker armature or to the shaker table is critical; it is required that the fixation of the specimen should not have any natural frequencies in the frequency range of testing. Usually, the base acceleration of the fixation is controlled in a closed loop. Experimental transfer functions are usually based on sine-sweep, impact or random excitation and can be compared to the results obtained by using the finite element model. Proper dynamic analysis usually requires Experimental Modal Analysis (EMA) [9].

The following section makes a critical analysis of the various testing methodologies encountered in the literature, which differ not only in terms of machines but also of specimen geometries, external loads and state of stress in the critical location. Throughout the text, the terms "testing method" and "testing system" define a specific combination of testing machine, specimen geometry and load set used to perform a fatigue test.

4. Fatigue Testing Systems

Various fatigue testing systems are proposed in the literature, often with significant differences. Some systems apply deterministic (harmonic) loads, and others apply random loadings. While reviewing the systems described in the literature, this section emphasizes several important features related to fatigue testing. These features include the type of machine, specimen geometries, imposed constrains, number of input needed in terms of force and/or torque and acceleration, random loadings acting on the specimen (e.g., axial, bending, torsion, bending–torsion and tension–torsion loadings) and resulting state of stress in the critical location (e.g., uniaxial and biaxial). All these features constitute the general classification criterion adopted to classify the testing systems; see Table 1. The table groups the various systems based on common or different characteristics. It also points out whether the multiaxial state of stress applied by the system is correlated or not. Additionally, mentioned in Table 1 is the distinction of the type of specimen (i.e., plate, cylindrical and more elaborated), which is discussed in more detail later on. The

classification criterion of Table 1 may represent a useful guideline to classify any new testing system.

Table 1. Classification of fatigue testing systems (C = correlated stress components; UC = uncorrelated stress components).

Machine	Specimen	Number of Inputs	Random Loading Applied to Specimen [1]					STATE OF STRESS IN Specimen			Ref.
			Ax	Be	To	Ax-To	Be-To	Uniaxial	Biaxial [2]	Biaxial [3]	
Servo-hydraulic	Plate	2	x					σ_{xx}	C		[33]
	Cylindrical	1 or 2	x		x	x		σ_{xx} or τ_{xy}		C or UC	[34]
Shaker tables	Plate	1		x				σ_{xx}			[10–14]
		1		x				σ_{xx}	C		[35–37]
	Cylindrical	1		x	x		x	σ_{xx} or τ_{xy}		C	[15]
		2		x	x		x	σ_{xx} or τ_{xy}		C or UC	[15]
		1		x			x	σ_{xx}		C	[16]
		1 or 2		x	x		x	σ_{xx} or τ_{xy}		C or UC	[17–19,38,39]
	More elaborated	1 or 2		x				σ_{xx}	UC		[20–25]

[1] Ax = axial; Be = bending; To = torsion; Ax-To = axial-torsion; Be-To = bending–torsion. [2] Biaxial with two normal stresses, σ_{xx} and σ_{yy}. [3] Biaxial with normal stress, σ_{xx}, and shear stress, τ_{xy}.

Electrodynamic shakers seem to be the most used machine, at least for the systems considered in Table 1. A possible reason for this is that the time to perform fatigue tests in high-cycle regime with random loadings is significantly shorter with shakers than servo-hydraulic machines. Another reason is that accelerated vibration tests in the automotive and aerospace industry are defined for electrodynamic shakers. Table 1 shows that the maximum number of excitations is two (e.g., vertical and horizontal accelerations), although some shakers allow three independent excitations to be applied simultaneously (e.g., vertical, horizontal and longitudinal acceleration)—in fact, only two of them are the active channels. Note also that servo-hydraulic machines in Table 1 are used to apply axial, torsion or axial-torsion loading, whereas shaker tables can apply bending, torsion or bending–torsion loadings. The type of state of stress in the specimen varies widely from one system to the other. However, cylindrical specimens can produce a pure shear stress, or combined normal and shear stresses, whereas the other specimen geometries cannot. Details of each type of specimen are described in the following sections.

4.1. Plate Specimens

Thin plate specimens with rectangular or square shape, excited at the base in vertical direction, represent the simplest and most convenient layout to produce a uniaxial state of stress in notches or holes; see [10–14] in Table 1. These systems are usually mounted on shaker tables and then excited by harmonic acceleration centered on the specimen resonant frequency. Harmonic acceleration has the advantage of easily obtaining the harmonic transfer function as the ratio between accelerations at two measurement positions. In fact, two accelerometers can be used [10–12], one attached on the base of the shaker and the second one attached at the free end of the specimen. A few accelerometers positioned along the entire length of the specimen are also observed in some applications [40,41] with the aim to obtain the modes of vibration at resonance frequencies. Although harmonic loadings allow the harmonic transfer function of the system to be determined, and they can also be used for constant amplitude fatigue tests, the random acceleration is the type of excitation most used in fatigue tests with shaker tables, so as to replicate the random loadings commonly found in engineering applications.

It is important to underline that plate specimens with rectangular or square shape, mounted on shaker tables and excited at the base, cannot produce a biaxial state of stress

at critical location, but rather a uniaxial stress state. This circumstance occurs even if the specimen is excited by a multiaxial input along more than one direction, for example, vertical and horizontal accelerations, each of which can produce a bending loading. Indeed, these plate specimens of thin thickness are usually subjected to bending loadings that lead to a uniaxial state of stress in the critical location.

Plate specimens with circular shape are also employed for tests with shaker tables [35,36]. As depicted in Figure 5, such specimens are fixed at the center and then excited by a vertical random acceleration, which produces a biaxial state of stress with the critical location outside the center. The intensity of stress components can be controlled by varying the diameter or thickness of the specimen. However, the nonzero stress components are only the radial and circumferential ones. Plate specimens with a circular shape then do not develop shear stress components at the critical point; see [35,36].
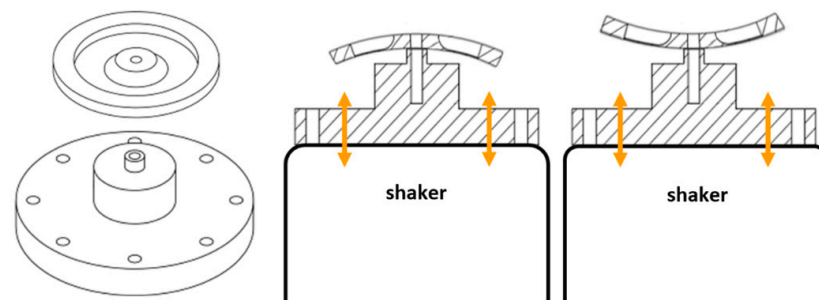

Figure 5. Testing system with a circular plate specimen excited by a uniaxial shaker (reprinted with permission from ref. [35]. Copyright 2021 Elsevier).

Plate specimens with cruciform geometry, excited by random loadings, are encountered in some fatigue tests using a servo-hydraulic machine; see [33,42] in Table 1. More often, this type of specimen is used in constant amplitude low cycle fatigue tests [43], whereas it seems not to be used in low cycle regime with random loadings.

When loaded by axial loadings applied to its two orthogonal arms (see Figure 6), the cruciform specimen can develop in the critical location a biaxial stress with two normal stress components, similarly to the circular plate specimen.
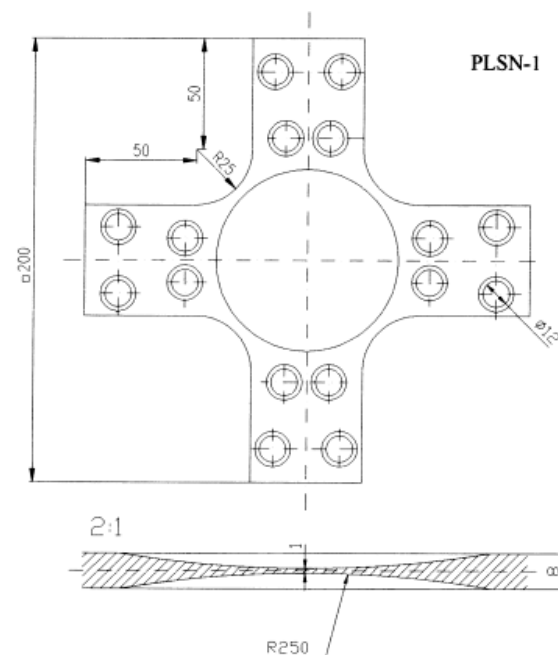
Figure 6. Plate specimens with cruciform geometry (reprinted with permission from ref. [33]. Copyright 1999 Elsevier).

Other plate specimen shapes (e.g., a particular wing shape) can be considered in tests if a biaxial stress is to be obtained by means of shaker tables; see [37] in Table 1. Though a plate specimen can develop a biaxial state of stress with two normal stresses, it cannot generate a biaxial state with normal and shear stresses. To obtain this stress, a cylindrical specimen is required.

4.2. Cylindrical Specimens

Cylindrical specimens, with or without notches, can be loaded in bending if excited by a vertical acceleration imposed by a shaker table. The acceleration can be harmonic or random, and the bending loading accordingly. In the typical layout, the specimen has one end free and the other fixed to the shaker table. The system may be instrumented by two or more accelerometers to measure accelerations at different points, and by strain gages attached on notches to control the strain [44].

In some applications, the above system is excited simultaneously by tri-axis excitations centered on specimen resonance frequencies [31,32]. Although the random loadings correspond to axial and to bending loadings in two planes, the state of stress remains uniaxial in the critical location of interest. Indeed, it is only the maximum stress position that changes, depending on the intensity and phase shift of the excitations. Therefore, the use of a tri-axial shaker does not assure that a biaxial state of stress be obtained on a cantilever cylindrical specimen. This example emphasizes that a different configuration of the test system is needed to reach a biaxial state of stress in cylindrical specimens.

To this end, a possible solution is to exploit a uniaxial shaker with a rotary table structure and a lever [15]. In one side, the cantilever cylindrical specimen is fixed to the holder structure; in the other side, it is attached to the lever. By rotating the lever arm with an arbitrary angle in the range $0 \leq \alpha \leq \pi/2$, the shaker excites the lever by imposing simultaneous bending and torsion moments to the specimen. Due to its layout, this system can only develop a coupled (correlated) bending–torsion loading, i.e., it is limited to proportional loadings. Accordingly, in Table 1, this system is listed in the fifth row (ref. [15], with one input). Choosing either of the two limit angular values, the system can apply a pure bending when the lever is parallel to the specimen axis ($\alpha = 0$), or a pure torsion when the lever is perpendicular to the specimen axis ($\alpha = \pi/2$). Strain gages are also attached on the lever to measure the strain and to control the value of normal stress

in the specimen. According to the imposed angle α, it is straightforward to calculate the value of stress in any system configuration, i.e., biaxial normal and shear stresses when $0 < \alpha < \pi/2$, uniaxial pure normal stress when $\alpha = \pi/2$ and uniaxial pure shear stress when $\alpha = 0$.

By adopting a similar system layout, fatigue tests can also be performed with uncoupled (uncorrelated) bending–torsion loadings [15]. In contrast to the system described so far, now two uniaxial shakers are controlled independently. They are mounted on a table in order to excite two arms positioned perpendicularly; see Figure 7. In this case, not only coupled but also uncoupled bending–torsion random loadings can be achieved. Accordingly, in Table 1, this system is listed in the sixth row (ref. [15], with two inputs). This system yields a pure bending loading when only the arm parallel to specimen axis is excited by a uniaxial shaker. Instead, if the excitation is only imposed by the other shaker (arm perpendicular to the specimen), the specimen is subjected to torsion loading, without bending. Of course, this testing system layout needs two uniaxial shakers. Furthermore, it requires an input/output system to control the accelerations in the two shakers simultaneously.

By adding two tip masses of different weight at the free end of a cylindrical specimen excited by a uniaxial shaker table, it is possible to obtain a bending–torsion loading in the specimen; see [16] in Table 1. This layout shows that a specimen excited by a base vertical random acceleration experiences a normal and shear biaxial stress. In this layout, however, both stress components are always coupled. Their relative magnitude can be controlled by increasing or decreasing the weight ratio of the two tip masses. A pure bending loading results by selecting the same weight for both tip masses. However, obtaining the opposite loading case (only torsion) is not possible—indeed, torsion is always coupled with bending. Another aspect to mention is that this layout seems not to have been verified by experimental tests, but only by numerical simulations [16].
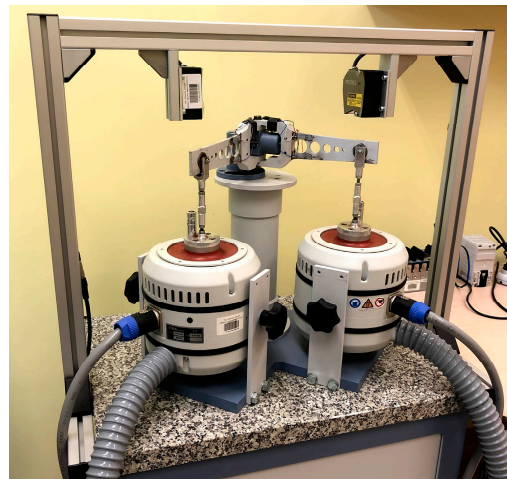

Figure 7. Testing system with a cylindrical specimen excited by two independent shakers.

A way to decouple the bending and torsion loadings—and thus improve the capabilities of the testing system in [16]—is to use a tri-axis shaker, which can apply up to three independent excitations along three orthogonal directions. Inspired by [16], a special holder structure (see Figure 8) has been designed to allow the bending and torsion random loadings to be controlled independently; see [17–19] in Table 1. In the system in Figure 8, a U-notched cylindrical specimen is fixed to a T-clamp at one end. At the other end, the specimen mounts a cantilever arm with two equal masses, and it is also constrained by a thin and flexible plate.
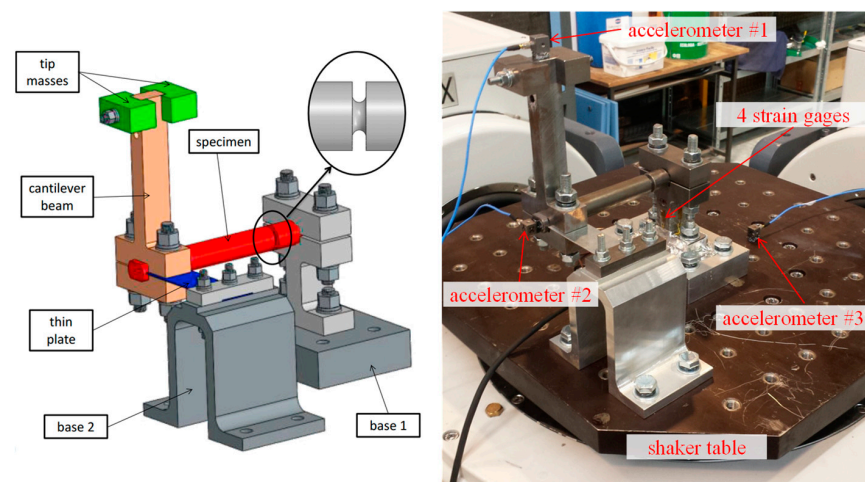
Figure 8. Testing system composed of a cylindrical specimen with eccentric tip masses, and excited by vertical and/or horizontal base accelerations (adapted with permission from ref. [19]. Copyright 2018 Elsevier).

This thin and flexible plate constraints any horizontal movement but allows the rotation of the specimen end. The plate thus prevents the specimen from being subjected to bending in horizontal direction, but it is very thin to allow the specimen to rotate around its axis when subjected to torsion. Therefore, when the specimen is excited by a vertical base acceleration, Figure 9a, it vibrates in the vertical plane (only bending loading). When, instead, it is excited by a horizontal base acceleration, Figure 9b, it vibrates in the horizontal plane (only torsion loading caused by the oscillation of the two eccentric masses).
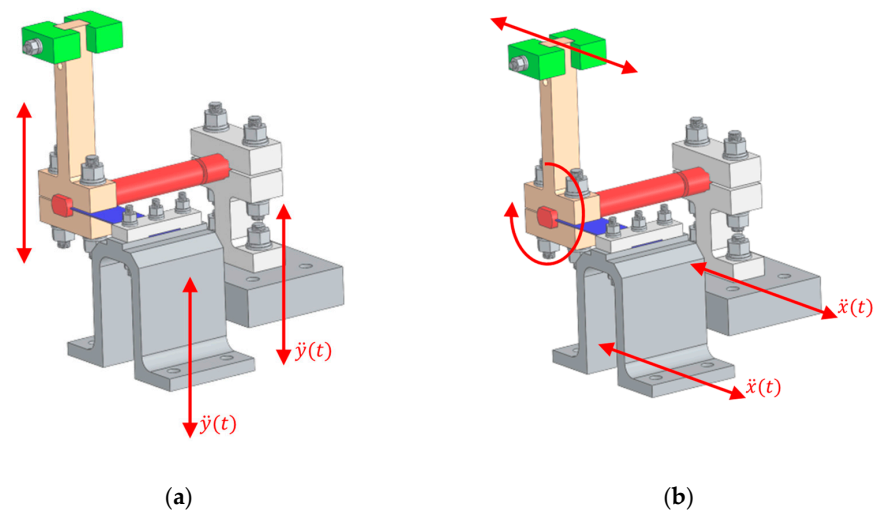

| (**a**) | (**b**) |

Figure 9. Testing system with a cylindrical specimen excited by (**a**) vertical base acceleration and (**b**) horizontal base acceleration.

The testing system has accelerometers to monitor the accelerations of the shaker table in closed-loop control, and the acceleration of the extremity of the specimen and cantilever arm. As it is not possible to use strain gages to measure the strains directly at the specimen notch (being it too small), an indirect measure it performed. Strain gages are indeed glued onto the lateral faces of the T-clamp, so as to provide a measure of the bending moments there and, indirectly, of the bending and torsion loadings and, accordingly, of the resulting normal and shear stress at the specimen notch.

Note that the tri-axis shaker cannot excite only one single axis or two axes at a time, keeping the others at rest. All three axes need to be active simultaneously, which appears to be a small limitation if tests with two, or even only one, accelerations need to be carried

out. However, this circumstance can easily be overcome by setting a very low level of acceleration on the "secondary" axes that, theoretically, should not be activated.

It is finally worth to mention that the system layout described so far, as shown in Figure 8, has been adopted in [38,39], though with two lateral thin plates instead of one, to perform bending–torsion fatigue tests.

Hollow cylindrical specimens subjected to axial, torsion and internal pressure perhaps represent the most versatile testing system in terms of the state of stress achievable. Indeed, this system allows a three-dimensional stress state (two normal stresses and one shear stress) to be obtained by servo-hydraulic machines and pressure chambers [45,46]. On the other hand, it may be presumed that loading a hollow specimen in axial, torsion and simultaneously with an internal pressure, requires special-purpose equipment that is likely to be more expensive than the usual testing machines found in laboratories.

A hollow cylindrical specimen with a small hole perpendicular to its axis, loaded by a servo-hydraulic machine, may be subjected to an uncoupled biaxial state of stress; see [34] in Table 1. This specimen is fixed at both ends, where the servo-hydraulic machine applies an axial-torsion random loading. The biaxial state of stress at the hole can be monitored with minimal difficulty by controlling the input force and/or torque and relating it to the corresponding stress components. Once again, this system configuration emphasizes how servo-hydraulic machines offer a greater simplicity over shaker tables in the direct control of both the intensity and phase shift between axial-torsion loading actions on cylindrical specimens. Instead, cantilever cylindrical specimens excited by shakers require the dynamic response of the specimen fixed on the holder system to be determined in order to evaluate the normal and shear stress values at the critical location.

4.3. More Elaborated Specimens

More elaborated specimens are developed with the aim to perform accelerated fatigue tests using shaker tables and simulate a real-world scenario of complex structures. A Y-shaped specimen with a central hole and two masses at the free ends has been proposed; see Figure 10. The Y-shaped specimen is made by three rectangular cross-sections arranged at 120° around the hole and has in the frequency range up to 2 kHz several natural frequencies that can be vibration fatigued. The attached masses can be used to adjust the frequencies of particular natural frequencies [21]. In [22], it was shown that the internal damping has a significant influence on the fatigue damage. In [20], multiaxial loads were achieved by exciting two mode shapes (one in the vertical and one in the horizontal direction). In vibration fatigue, the specimen is typically considered as broken when the natural frequency drops by 2–5% (different values are used in different studies); see e.g., [9]. Fatigue parameters (fatigue strength and inverse slope of S–N curve) need to be experimentally identified using the specimen; see e.g., [23], where 10 specimens were used. It may finally be presumed that manufacturing several specimens with more elaborated geometry has a cost slightly higher than producing specimens with simpler shapes.
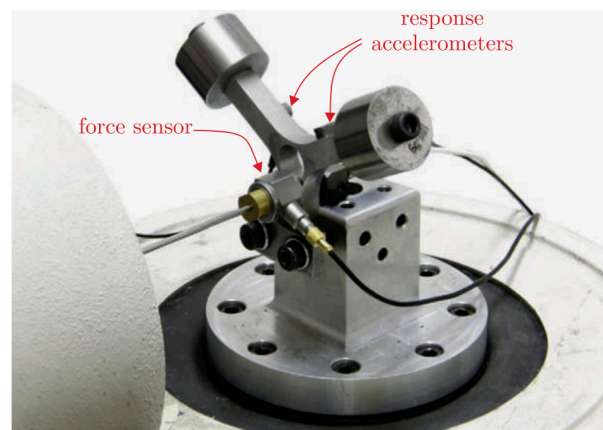
Figure 10. Testing system including Y-shaped specimen with a central hole and two masses at the free ends subjected to horizontal force and vertical acceleration (reprinted with permission from ref. [23]. Copyright 2016 Elsevier).

In [20], two electrodynamic shakers were used: one for vertical random excitation (for the excitation of first natural frequency) and one for horizontal excitation (for the second natural frequency). Masses attached to the Y-sample allowed modal frequencies to be adjusted to the needs. The test system is instrumented with accelerometers positioned at different points and a strain gage attached in the critical region. The accelerometers are used to monitor in real time the dynamic response of system, which in turn updates the FE model. The vertical excitations are controlled in a closed loop with measurements of accelerometers. Another excitation is applied perpendicular to the shaker vertical axis. It is imposed close to the specimen hole and monitored by a force transducer.

This special Y-shaped system is excited by two uncoupled random loadings (along vertical and horizontal directions); see [20–25] in Table 1. The system can develop an uncoupled biaxial state of stress at the critical location in terms of normal stress components.

5. Conclusions

This paper presented an overview of the various fatigue testing systems used for subjecting metals to random loadings, as they are described in relevant articles from the literature. The presented overview of relevant works compared the different testing systems in terms of several characteristics, namely, the type of machine (e.g., servo-hydraulic and shaker tables), specimen geometry, number of inputs needed to carry out a fatigue test, random loadings acting on the specimen and resulting local state of stress. For each of the above characteristics, Table 2 summarizes the specific features adopted for classifying the various systems. Based on the specific features in Table 2, all the analyzed testing systems were also classified into a more comprehensive table (named Table 1 in the text), which allowed the analogies, differences, advantages and possible limitations to be emphasized in a clear way. Both tables also summarize the main criteria that may be used, in the future, as a guideline to classify new equipment.

Table 2. Characteristics and specific features used to classify fatigue testing systems.

Machine	Specimen Geometry	Random Loading [1]	State of Stress
Servo-hydraulic orshaker table	Plate, cylindrical or more elaborated	Ax, Be, To, Ax-To or Be-To	Uniaxial, biaxial with σ_{xx} and σ_{yy} or biaxial with σ_{xx} and τ_{xy}

[1] Ax = axial; Be = bending; To = torsion; Ax-To = axial-torsion; Be-To = bending–torsion.

Conflicts of Interest: The authors declare no conflict of interest.

References

1. Benasciutti, D. *Fatigue Analysis of Random Loadings: A Frequency Domain Approach*; LAP Lambert Academic Publishing: Saarbrücken, Germany, 2012; ISBN 9783659123702.
2. Benasciutti, D.; Sherratt, F.; Cristofori, A. Recent developments in frequency domain multi-axial fatigue analysis. *Int. J. Fatigue* **2016**, *91*, 397–413. [CrossRef]
3. Du, J.; Li, H.; Zhang, M.; Wang, S. A novel hybrid frequency-time domain method for the fatigue damage assessment of offshore structures. *Ocean Eng.* **2015**, *98*, 57–65. [CrossRef]
4. Li, Z.; Ringsberg, J.W.; Storhaug, G. Time-domain fatigue assessment of ship side-shell structures. *Int. J. Fatigue* **2013**, *55*, 276–290. [CrossRef]
5. Kocabicak, U.; Firat, M. A simple approach for multiaxial fatigue damage prediction based on FEM post-processing. *Mater. Des.* **2004**, *25*, 73–82. [CrossRef]
6. Marques, J.M.E.; Benasciutti, D.; Carpinteri, A.; Spagnoli, A. An algorithm for fast critical plane search in computer-aided engineering durability analysis under multiaxial random loadings: Application to the Carpinteri–Spagnoli–Vantadori spectral method. *Fatigue Fract. Eng. Mater. Struct.* **2020**, *43*, 1978–1993. [CrossRef]
7. Benasciutti, D.; Marques, J.M.E. An efficient procedure to speed up critical plane search in multiaxial fatigue: Application to the Carpinteri-Spagnoli spectral criterion. *MATEC Web Conf.* **2019**, *300*, 16003. [CrossRef]
8. Mršnik, M.; Slavič, J.; Boltežar, M. Vibration fatigue using modal decomposition. *Mech. Syst. Signal Process.* **2018**, *98*, 548–556. [CrossRef]
9. Slavič, J.; Boltežar, M.; Mršnik, M.; Česnik, M.; Javh, J. *Vibration Fatigue by Spectral Methods: From Structural Dynamics to Fatigue Damage-Theory and Experiments*, 1st ed.; Elsevier: Amsterdam, The Netherlands, 2020; ISBN 9780128221907.
10. Khalij, L.; Gautrelet, C.; Guillet, A. Fatigue curves of a low carbon steel obtained from vibration experiments with an electrodynamic shaker. *Mater. Des.* **2015**, *86*, 640–648. [CrossRef]
11. Gautrelet, C.; Khalij, L.; Appert, A.; Serra, R. Linearity investigation from a vibratory fatigue bench. *Mech. Ind.* **2019**, *20*, 101. [CrossRef]
12. Appert, A.; Gautrelet, C.; Khalij, L.; Troian, R. Development of a test bench for vibratory fatigue experiments of a cantilever beam with an electrodynamic shaker. *MATEC Web Conf.* **2018**, *165*, 10007. [CrossRef]
13. Ellyson, B.; Brochu, M.; Brochu, M. Characterization of bending vibration fatigue of SLM fabricated Ti-6Al-4V. *Int. J. Fatigue* **2017**, *99*, 25–34. [CrossRef]
14. Ghielmetti, C.; Ghelichi, R.; Guagliano, M.; Ripamonti, F.; Vezzù, S. Development of a fatigue test machine for high frequency applications. *Procedia Eng.* **2011**, *10*, 2892–2897. [CrossRef]
15. Łagoda, T.; Macha, E.; Niesłony, A. Fatigue life calculation by means of the cycle counting and spectral methods under multiaxial random loading. *Fatigue Fract. Eng. Mater. Struct.* **2005**, *28*, 409–420. [CrossRef]
16. Nguyen, N.; Bacher-Höchst, M.; Sonsino, C.M. A frequency domain approach for estimating multiaxial random fatigue life. *Mater. Werkst.* **2011**, *42*, 904–908. [CrossRef]
17. Zanellati, D.; Benasciutti, D.; Tovo, R. Vibration fatigue tests by tri-axis shaker: Design of an innovative system for uncoupled bending/torsion loading. *Procedia Struct. Integr.* **2018**, *8*, 92–101. [CrossRef]
18. Zanellati, D.; Benasciutti, D.; Tovo, R. Fatigue strength of S355JC steel under harmonic and random bending-torsion loading by a tri-axis shaker: Preliminary experimental results. *MATEC Web Conf.* **2019**, *300*, 17006. [CrossRef]
19. Zanellati, D.; Benasciutti, D.; Tovo, R. An innovative system for uncoupled bending/torsion tests by tri-axis shaker: Numerical simulations and experimental results. *MATEC Web Conf.* **2018**, *165*, 16006. [CrossRef]
20. Česnik, M.; Slavič, J.; Čermelj, P.; Boltežar, M. Frequency-based structural modification for the case of base excitation. *J. Sound Vib.* **2013**, *332*, 5029–5039. [CrossRef]
21. Ogrinec, P.; Slavič, J.; Česnik, M.; Boltežar, M. Vibration fatigue at half-sine impulse excitation in the time and frequency domains. *Int. J. Fatigue* **2019**, *123*, 308–317. [CrossRef]
22. Palmieri, M.; Česnik, M.; Slavič, J.; Cianetti, F.; Boltežar, M. Non-Gaussianity and non-stationarity in vibration fatigue. *Int. J. Fatigue* **2017**, *97*, 9–19. [CrossRef]
23. Mršnik, M.; Slavič, J.; Boltežar, M. Multiaxial vibration fatigue—A theoretical and experimental comparison. *Mech. Syst. Signal Process.* **2016**, *76–77*, 409–423. [CrossRef]
24. Mršnik, M.; Slavič, J.; Boltežar, M. Multiaxial Fatigue Criteria for Random Stress Response–Theoretical and Experimental Comparison. *Procedia Eng.* **2015**, *101*, 459–466. [CrossRef]
25. Česnik, M.; Slavič, J.; Boltežar, M. Uninterrupted and accelerated vibrational fatigue testing with simultaneous monitoring of the natural frequency and damping. *J. Sound Vib.* **2012**, *331*, 5370–5382. [CrossRef]
26. Susmel, L. *Multiaxial Notch Fatigue*, 1st ed.; Woodhead Publishing: Cambridge, UK, 2009; ISBN 9781845695828.
27. Morettini, G.; Braccesi, C.; Cianetti, F.; Razavi, S.M.J.; Solberg, K.; Capponi, L. Collection of experimental data for multiaxial fatigue criteria verification. *Fatigue Fract. Eng. Mater. Struct.* **2019**, *43*, 162–174. [CrossRef]
28. Socie, D.; Marquis, G. *Multiaxial Fatigue*; SAE International: Warrendale, PA, USA, 2000; ISBN 9780768065107.

29. Benasciutti, D.; Zanellati, D.; Cristofori, A. The "Projection-by-Projection" (PbP) criterion for multiaxial random fatigue loadings. *Frattura Integrità Strutt.* **2018**, *13*, 348–366. [CrossRef]

30. Pilkey, W.D.; Pilkey, D.F. *Peterson's Stress Concentration Factors*, 3rd ed.; John Wiley & Sons: Hoboken, NJ, USA, 2008; ISBN 978047004824.

31. Luo, Z.; Chen, H.; He, X.; Zheng, R. Two time domain models for fatigue life prediction under multiaxial random vibrations. *Proc. Inst. Mech. Eng. Part C J. Mech. Eng. Sci.* **2019**, *233*, 4707–4718. [CrossRef]

32. Whiteman, W.E.; Berman, M.S. Fatigue failure results for multi-axial versus uniaxial stress screen vibration testing. *Shock Vib.* **2002**, *9*, 319–328. [CrossRef]

33. Łagoda, T.; Macha, E.; Bedkowski, W. A critical plane approach based on energy concepts: Application to biaxial random tension-compression high-cycle fatigue regime. *Int. J. Fatigue* **1999**, *21*, 431–443. [CrossRef]

34. Niesłony, A.; Růžička, M.; Papuga, J.; Hodr, A.; Balda, M.; Svoboda, J. Fatigue life prediction for broad-band multiaxial loading with various PSD curve shapes. *Int. J. Fatigue* **2012**, *44*, 74–88. [CrossRef]

35. Morettini, G.; Braccesi, C.; Cianetti, F.; Razavi, S. Design and implementation of new experimental multiaxial random fatigue tests on astm-a105 circular specimens. *Int. J. Fatigue* **2021**, *142*, 105983. [CrossRef]

36. Morettini, G.; Braccesi, C.; Cianetti, F. Experimental multiaxial fatigue tests realized with newly developed geometry specimens. *Fatigue Fract. Eng. Mater. Struct.* **2018**, *42*, 827–837. [CrossRef]

37. George, T.J.; Seidt, J.; Shen, M.-H.H.; Nicholas, T.; Cross, C.J. Development of a novel vibration-based fatigue testing methodology. *Int. J. Fatigue* **2004**, *26*, 477–486. [CrossRef]

38. Luo, Z.; Chen, H.; He, X. Influences of correlations between biaxial random vibrations on the fatigue lives of notched metallic specimens. *Int. J. Fatigue* **2020**, *139*, 105730. [CrossRef]

39. Luo, Z.; Chen, H.; Zheng, R.; Zheng, W. A damage gradient model for fatigue life prediction of notched metallic structures under multiaxial random vibrations. *Fatigue Fract. Eng. Mater. Struct.* **2020**, *43*, 2101–2115. [CrossRef]

40. Kim, C.-J.; Lee, B.-H.; Kang, Y.J.; Ahn, H.-J. Accuracy enhancement of fatigue damage counting using design sensitivity analysis. *J. Sound Vib.* **2014**, *333*, 2971–2982. [CrossRef]

41. Kim, C.-J.; Kang, Y.J.; Lee, B.-H.; Ahn, H.-J. Design sensitivity analysis of a system under intact conditions using measured response data. *J. Sound Vib.* **2012**, *331*, 3213–3226. [CrossRef]

42. Aid, A.; Bendouba, M.; Aminallah, L.; Amrouche, A.; Benseddiq, N.; Benguediab, M. An equivalent stress process for fatigue life estimation under multiaxial loadings based on a new non linear damage model. *Mater. Sci. Eng. A* **2012**, *538*, 20–27. [CrossRef]

43. Itoh, T.; Sakane, M.; Ohnami, M. High temperature multiaxial low cycle fatigue of cruciform specimen. *J. Eng. Mater. Technol.* **1994**, *116*, 90–98. [CrossRef]

44. Kim, C.–J.; Kang, Y.J.; Lee, B.–H. Experimental spectral damage prediction of a linear elastic system using acceleration response. *Mech. Syst. Signal. Process.* **2011**, *25*, 2538–2548. [CrossRef]

45. Papuga, J.; Fojtík, F. Multiaxial fatigue strength of common structural steel and the response of some estimation methods. *Int. J. Fatigue* **2017**, *104*, 27–42. [CrossRef]

46. Fojtík, F.; Papuga, J.; Fusek, M.; Halama, R. Validation of multiaxial fatigue strength criteria on specimens from structural steel in the high-cycle fatigue region. *Materials* **2020**, *14*, 116. [CrossRef] [PubMed]